Green Chemistry

PAPER

View Article Online
View Journal | View Issue

Open Access Article. Published on 31 October 2024. Downloaded on 1/15/2026 1:54:23 AM.
This article is licensed under a Creative Commons Attribution-NonCommercial 3.0 Unported Licence.

Check for updates

Cite this: *Green Chem.*, 2024, **26**, 11976

CO_2 catalyzed recycling of polyester and polycarbonate plastics†

Qiao Zhang,[a] Nan Wang,[a,b] Chenyang Hu,[a] Peng-Yuan Li,[c] Fu-Quan Bai,[c,d] Xuan Pang,*[a,b] Xuesi Chen[a,b] and Xianhong Wang[a]

Received 24th September 2024,
Accepted 30th October 2024

DOI: 10.1039/d4gc04782f

rsc.li/greenchem

Recycling waste polymeric materials is essential for environmental protection and achieving carbon neutrality. This study demonstrates the efficacy of CO_2 as a metal-free catalyst for the chemical recycling of common waste polyester and polycarbonate plastics *via* alcoholysis to yield valuable organic chemicals. CO_2 was proposed to act as a Lewis acid–base pair, activating both alcohol and ester (carbonate) functional groups during the catalytic process. The depolymerization mechanism was thoroughly investigated by monitoring conversion rates and changes in M_n values. Pre-treatment of the polymer materials in THF was found to accelerate the depolymerization rate. End-of-life waste materials were completely degraded into valuable organic molecules, irrespective of their physical and chemical properties. Unlike conventional solid and liquid catalysts, CO_2 leaves no residue in the final products. Moreover, this work unveils the catalytic role for CO_2, expanding its traditional function as a C1 building block in synthetic chemistry.

Introduction

Plastics are indispensable to modern life and serve as crucial engineering materials. Annual global plastic production reached 390 million tons in 2016. This number is projected to climb to 780 million tons by 2036 and 1.2 billion tons by 2060.[1,2] Yet approximately 150 million tons of plastic waste are generated each year.[3] Regrettably, only about one-fifth of this waste is recycled, with the majority ending up in landfills or oceans.[4] As plastic consumption grows, so too does the environmental crisis. Improperly disposed plastic waste is non-biodegradable, contaminating the biosphere. Plastic bags and bottles pose a significant threat to wildlife, causing ingestion and digestive problems. Microplastics, derived from shredded plastic waste, have been linked to human health issues.[5] Given these challenges, effective waste plastic management is imperative for individuals, the environment, and the global community.

Several methods exist for deconstructing and recycling plastic waste. Incineration, while a simple process for reducing waste volume and recovering energy through combustion, yields worthless and unrecoverable small molecules like H_2O, CO_2, N_2, and NO_x. Mechanical recycling, involving sorting, cleaning, shredding, melting, and reforming, is straightforward but struggles with contamination and quality degradation, limiting the applications of recycled materials.[6,7] Biodegradation presents a sustainable alternative to traditional plastics.[8] Driven by increasing demand, production of biodegradable polymers is expected to soar from 1.09 million tons in 2019 to 1.80 million tons by 2025.[9] Polylactide (PLA), a biodegradable aliphatic polyester, exemplifies this category, comprising one-third of global biodegradable polymer production. While biodegradable polymers present an environmentally friendly option compared to traditional plastics like polyolefin, they often require lengthy decomposition times and produce unrecoverable end products *e.g.* H_2O and CO_2.

In addition to incineration, mechanical recycling, and biodegradation, chemical recycling offers a promising approach to polymer deconstruction. This process involves controlled reactions to break down polymers into oligomers and monomers.[10] For PLA specifically, alcoholysis,[11–18] hydrolysis,[19–21] aminolysis,[22–25] and hydrogenolysis[26–30] have been explored. Among these methods, alcoholysis of PLA yields alkyl lactate, a product currently valued at 1.5 to 2 times the price of virgin PLA resins.[14] Moreover, alkyl lactate serves as a sustainable solvent in various chemical syntheses.[31,32]

Our team has previously reported the alcoholysis of PLA, as well as other polyester and polycarbonate materials, facilitated by various catalysts[33,34] or aprotic polar solvents.[35] We hypothesized that a Lewis acid–base pair is essential for activating

[a]*Key Laboratory of Polymer Ecomaterials, Changchun Institute of Applied Chemistry, Chinese Academy of Sciences, 5625 Renmin Street, Changchun 130022, China. E-mail: xpang@ciac.ac.cn; Tel: (+86) 431 85262588*
[b]*University of Science and Technology of China, Hefei 230026, China*
[c]*Institute of Theoretical Chemistry, College of Chemistry, Jilin University, Changchun 130023, China*
[d]*Chongqing Research Institute, Jilin University, Chongqing 401120, China*

†Electronic supplementary information (ESI) available: Experimental section, NMR spectra, *etc.* See DOI: https://doi.org/10.1039/d4gc04782f

This journal is © The Royal Society of Chemistry 2024

Open Access Article. Published on 31 October 2024. Downloaded on 1/15/2026 1:54:23 AM.
This article is licensed under a Creative Commons Attribution-NonCommercial 3.0 Unported Licence.

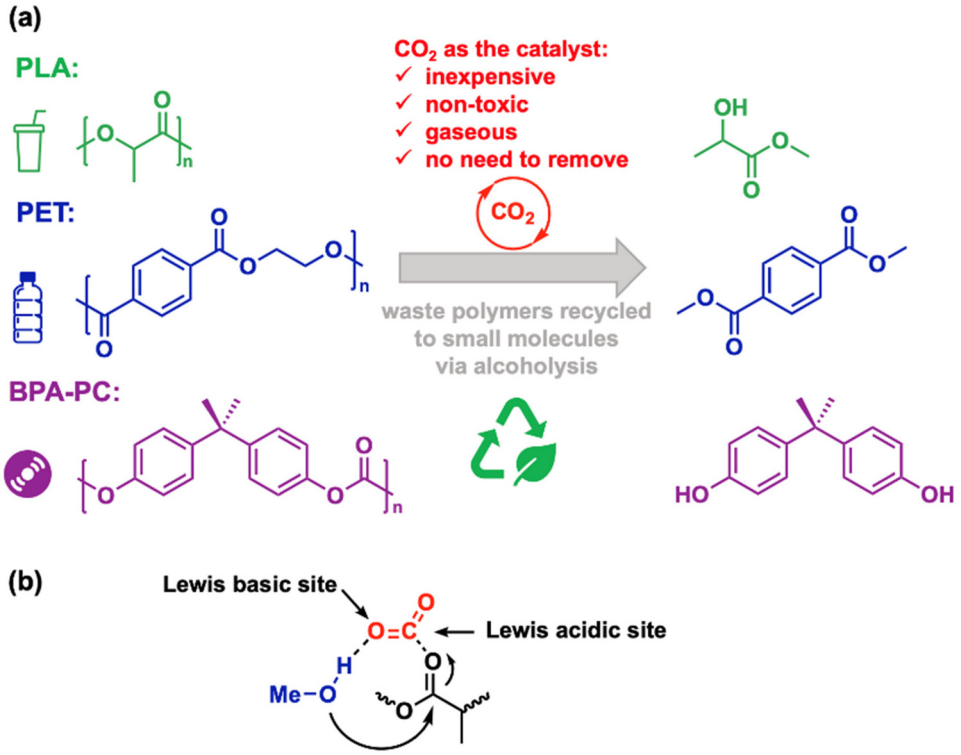

Scheme 1 (a) CO_2 catalyzed depolymerization and recycling waste polyesters and polycarbonates; (b) CO_2 as a Lewis acid–base pair for activating MeOH and polyester.

both alcohol and ester (or carbonate) groups within these polymers. Building upon our prior work, here we propose that the carbon atom in CO_2 acts as a Lewis acid, activating carbonyl groups in polyesters, while the oxygen atom in CO_2 serves as a Lewis base, activating alcohols. Based on this hypothesis, we explored the depolymerization of common waste polyester and polycarbonate materials through CO_2-catalyzed alcoholysis—an unconventional approach in catalysis (Scheme 1).

CO_2 is often recognized as a sustainable C1 building block capable of replacing toxic carbon sources like CO and phosgene in organic and polymer synthesis.[36,37] However, employing CO_2 as a metal-free catalyst remains challenging.[38] For instance, List *et al.* described CO_2-assisted α-allylation of ketones using palladium and a chiral phosphoric acid catalyst.[39] Young *et al.* explored CO_2-mediated C–H arylation of amines by utilizing CO_2 as an amine protecting and directing group.[40,41] Rovis, Schoenebeck, and colleagues investigated the direct α-alkylation of primary aliphatic amines, where CO_2 forms an *in situ* carbamate to accelerate C–H activation.[42] Additionally, Li, Wang, and co-workers reported Cl_2 evolution through NaCl electrolysis using an amide-containing organocatalyst and CO_2.[43] While these outstanding examples showcase CO_2 involvement, they necessitate additional catalysts, reagents, or external stimuli. In contrast, our research focuses on utilizing CO_2 as a standalone catalyst for a specific reaction, eliminating the need for catalyst removal as the gaseous CO_2 can be readily released.[44–47] Beyond PLA, we extended our investigation to the depolymerization of widely used polyethylene terephthalate (PET)[48,49] and bisphenol A based polycarbonate (BPA-PC).[50] Our work not only explores the fundamental catalytic role of CO_2 for activating alcohol and polymers, but also translates this knowledge into practical applications for recycling waste plastics, offering a sustainable approach to materials management.

Results and discussion

Initial investigations focused on evaluating the catalytic reactivity of CO_2. PLA resin R190 (M_n = 98.1 kg mol^{-1}, $Đ$ = 1.66) served as the starting material. Control experiments confirmed negligible methanolysis without a catalyst at 140 °C in methanol (Table 1, entry 1). However, under 1 MPa CO_2 pressure in a stainless-steel autoclave, 90% of PLA resins were degraded within 6 hours. Complete degradation achieved within 8 hours (Table 1, entry 2). ^{1}H NMR spectroscopy identified methyl lactate as the sole product, and 88% isolated yield was obtained by distillation. This unexpected result highlighted the efficacy of CO_2 as a catalyst for PLA alcoholysis. The ethanolysis of PLA required a longer reaction time due to a higher activation energy (Table S1†).[51] The influence on CO_2 pressure on the depolymerization rate was listed in Table S2.† Note that the reaction conditions employed were below the supercritical point of CO_2 (T_c = 31 °C and p_c = 7.4 MPa).[52] Importantly, CO_2

Open Access Article. Published on 31 October 2024. Downloaded on 1/15/2026 1:54:23 AM.
This article is licensed under a Creative Commons Attribution-NonCommercial 3.0 Unported Licence.

Table 1 CO_2 catalyzed methanolysis of PLA materials[a]

Entry	PLA material	Cat.	t (h)	Conv.[b] (%)	Methyl lactate : dimer ratio[b]
1	R190 resin	N/A	6	Trace	N/A
2	R190 resin	CO_2	6	90	91 : 9
			8	100	100 : 0
3	R290 resin	CO_2	6	43	54 : 46
			12	100	100 : 0
4	4032D resin	CO_2	6	100	100 : 0

[a] Reaction conditions: each reaction was carried out in a 25 mL stainless-steel autoclave. PLA material (288 mg, containing 4 mmol ester bonds), MeOH (3.2 g, 100 mmol, 25 equivalents relative to PLA ester bonds), CO_2 (1 MPa), T = 140 °C. [b] Conversion and percentage of dimers were determined by ^{1}H NMR spectroscopy (300 MHz, in $CDCl_3$).

consistently catalyzed the degradation of various commercial PLA resins irrespective of grade, size, or manufacturer (Table 1, entries 3 and 4). Unlike traditional solid or liquid catalysts, CO_2 leaves no catalyst contamination in the final product, eliminating the need for post-reaction catalyst removal. This advantage may also enable the recycling of waste PLA into novel PLA-based polymer materials.[53,54] Chiral stationary phase gas chromatography determined the chirality of the depolymerized product from PLLA. The product was confirmed as methyl L-lactate (Fig. S1†). Moreover, green metrics were calculated for the depolymerization process.[55,56] The atom economy (AE) was 100%. Environmental factor (e-factor) was 7.38, and process mass intensity (PMI) was 8.38, primarily due to the excess amount of MeOH used (Table S3†).

To elucidate the mechanism underlying PLA alcoholysis, we employed methyl lactate as a simplified model of the polymeric chain, reacting it with methanol-d_4 (CD_3OD) in the presence of CO_2. Fig. 1 presents the ^{1}H NMR spectroscopic characterization of the transesterification between methyl lactate and CD_3OD. In the absence of CO_2, only 21% conversion was observed after a 6-hour reaction at 140 °C (Fig. 1b). In contrast, CO_2 catalysis significantly enhanced the reaction, achieving a 92% conversion rate under identical conditions (Fig. 1c). The organic mimic reactions strongly suggest that CO_2 catalyzes PLA depolymerization through a transesterification mechanism. Furthermore, ^{2}H NMR spectroscopy revealed a signal increase at 3.13 ppm, corresponding to deuterated methyl lactate (Fig. S2†).

Transesterification between ethyl acetate and methanol serves as a model for PLA alcoholysis. Computational analysis reveals the catalytic role of CO_2 in this process (Fig. 2). In pathway 1, CO_2 catalyzes the reaction by forming a six-membered ring intermediate. The carbon in CO_2 acts as a Lewis acid, binding to the ester carbonyl, while the oxygen in CO_2 functions as a Lewis base, interacting with the hydrogen in methanol. This dual activation by CO_2 lowers the energy barrier to ΔG = 13.5 kcal mol^{-1} in transition state 1 (**TS-1**) and 8.7 kcal mol^{-1} in **TS-2**. Pathway 2, proceeding without a catalyst, involves two methanol molecules forming a six-membered

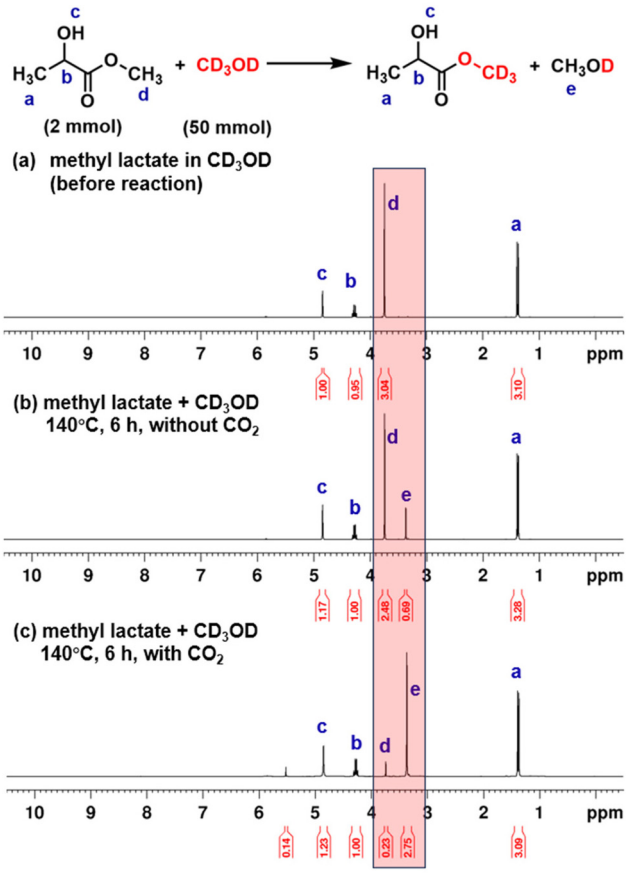

Fig. 1 ^{1}H NMR spectra of transesterification between methyl lactate and CD_3OD.

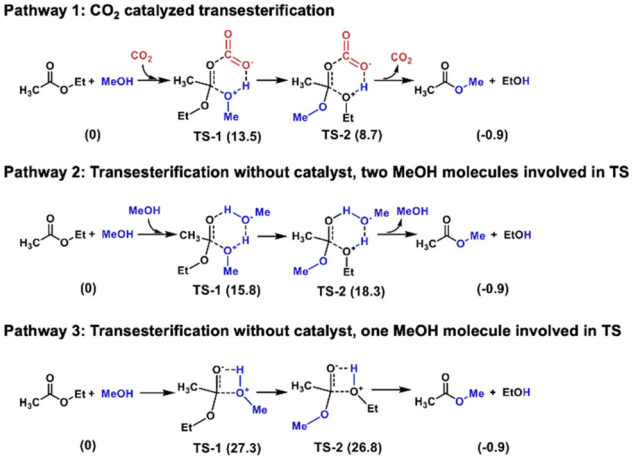

Fig. 2 Computational analysis of the transesterification between ethyl acetate and methanol. Numbers in parentheses represent energy changes in kcal mol^{-1}.

ring transition state, requiring higher activation energy with ΔG = 15.8 kcal mol^{-1} and 18.3 kcal mol^{-1} in **TS-1** and **TS-2**, respectively. Pathway 3, also catalyst-free, involves only one methanol molecule in a four-membered ring transition state

Open Access Article. Published on 31 October 2024. Downloaded on 1/15/2026 1:54:23 AM.
This article is licensed under a Creative Commons Attribution-NonCommercial 3.0 Unported Licence.

with ΔG = 27.3 kcal mol^{-1} and 26.8 kcal mol^{-1} in **TS-1** and **TS-2**, respectively, resulting in the highest energy barrier among the three pathways.

The kinetics of PLA methanolysis were investigated by monitoring methyl lactate formation and changes in M_n values during the depolymerization process (Fig. 3). Methyl lactate conversion was determined *via* ^{1}H NMR spectroscopy. Initially, the depolymerization rate was slow, likely due to the reaction being confined to the surface of PLA resin. After 4 hours, the rate accelerated as the resin was progressively degraded into shorter polymer chains and oligomers. Gel permeation chromatography (GPC) was employed to track M_n changes. In contrast to the initial slow depolymerization, M_n values decreased rapidly within the first 2 hours, dropping from 98.1 to 2.6 kg mol^{-1}. This dramatic decrease indicates a random chain scission mechanism rather than a stepwise depolymerization from the polymer chain end.

A plausible mechanism for CO_2-catalyzed depolymerization is outlined in Scheme 2. CO_2 functions as a Lewis acid–base pair, with the carbon atom acting as a Lewis acid to activate ester carbonyls and the oxygen atom acting as a Lewis base to activate the proton in methanol. In the transesterification process, methanol is thought as a nucleophile attacking the activated carbonyl group in the polyester. Subsequent ester bond cleavage leads to depolymerization, ultimately yielding methyl lactate as the final product.

Beyond PLA, we extended our research to the depolymerization of PET, the most consumed polyester in the world.[57] With excellent thermal and tensile properties,[58] PET finds extensive applications in textiles, packaging, and electronics. While chemical recycling of PET typically involves hydrolysis, alcoholysis, or glycolysis. These processes often require high temperatures due to PET's aromatic nature. Previous studies on PET

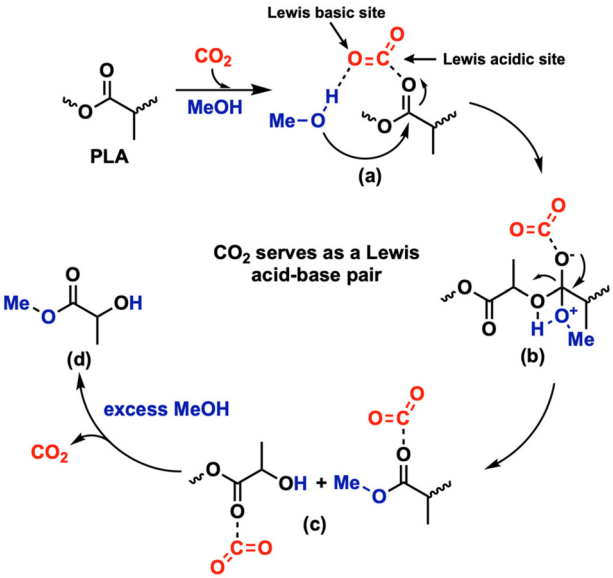

Scheme 2 A plausible mechanism for CO_2 catalyzed methanolysis of PLA.

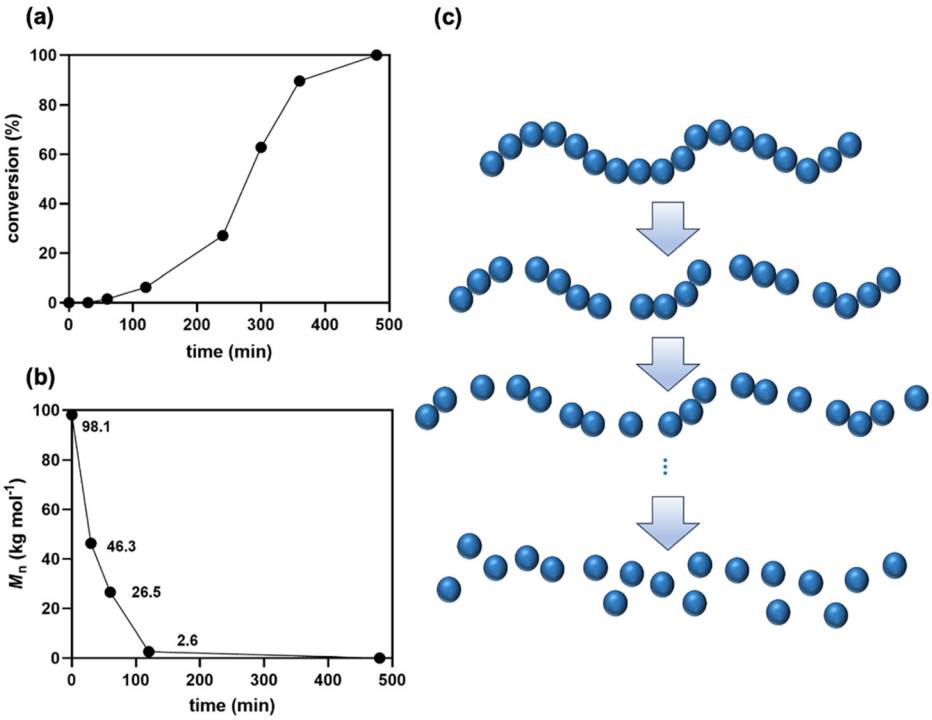

Fig. 3 Changes in (a) conversion and (b) M_n values for methanolysis of PLA resin R190 catalyzed by CO_2. (c) A scheme for the depolymerization mode of PLA (random chain scission).

Open Access Article. Published on 31 October 2024. Downloaded on 1/15/2026 1:54:23 AM.
This article is licensed under a Creative Commons Attribution-NonCommercial 3.0 Unported Licence.

methanolysis have relied on metal catalysts *e.g.*, Zn[59] and Ti[60] based catalyst. In this work, we explored the potential of CO_2 as a catalyst for converting PET to dimethyl terephthalate (DMT) *via* methanolysis. In the absence of CO_2, PET pellets remained unchanged (Table 2, entry 1). However, under CO_2 catalysis, complete depolymerization of PET pellets was achieved (Table 2, entry 3). Unlike the insoluble PET pellets, the product exhibited solubility in methanol and was amenable to removing solvent *in vacuo* with 83% isolated yield. ^{1}H NMR spectroscopy confirmed the formation of DMT (Fig. S9†).

Our third objective was to employ CO_2 catalysis for the depolymerization of BPA-PC, another widely consumed plastic. Renowned for its toughness, strength, and transparency, BPA-PC finds extensive applications in data storage, automotive and aircraft components, electronics, and construction.[57] Although the repeating unit is a carbonate rather than an ester, we hypothesized that the methanolysis mechanism for polycarbonate would resemble that of polyester. Indeed, we observed significant differences in reaction rates with and without CO_2 catalysis. Without CO_2 as catalyst, only 14% conversion was achieved at 140 °C after 6 hours (Table 2, entry 4). In contrast, CO_2 catalysis boosted conversion to 89% under identical conditions (Table 2, entry 5). Lowering the temperature to 120 °C virtually eliminated depolymerization (Table 2, entry 6). Consequently, we investigated CO_2-catalyzed methanolysis of BPA-PC pellets, monitoring the process hourly *via* ^{1}H NMR spectroscopy. Fig. 4 revealed minimal BPA formation during the initial 2 hours, likely due to the reaction being confined to the pellet surface. At the 3-hour mark, a significant increase in BPA signals was observed as the pellets disintegrated into powder, substantially increasing the surface area. Some incomplete degradation products were also detected.[61] After 6 hours, most of the BPA-PC had been converted to BPA. The isolated yield was 82% by removing solvent *in vacuo*.

To expedite the depolymerization process, we explored the effects of pre-treatment of polymeric materials with a solvent like tetrahydrofuran (THF).[62] Dissolution or swelling with THF can facilitate greater interaction with methanol. In our experiments, polymeric materials, including PLA, PET, and BPA-PC, were initially treated with THF for 1 hour at 65 °C to induce either dissolution (for PLA and BPA-PC) or swelling (for PET) prior to CO_2-catalyzed methanolysis (Fig. 5). We observed that pre-treatment significantly accelerated depolymerization com-

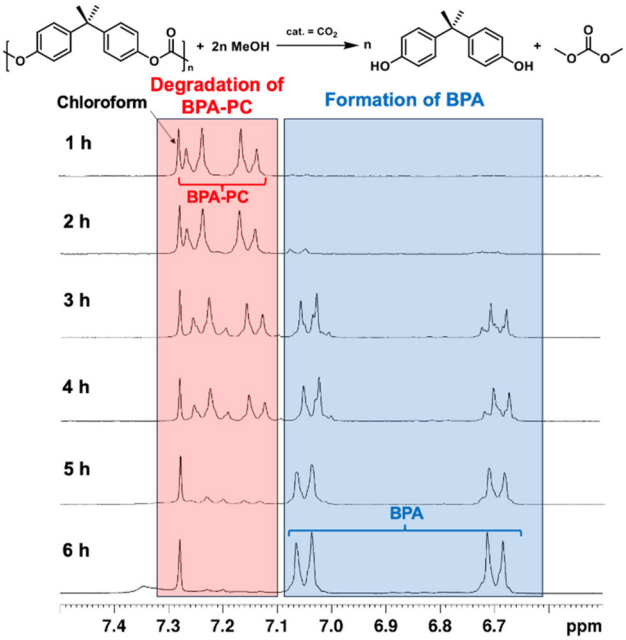

Fig. 4 CO_2 catalyzed methanolysis of the BPA-PC pellets monitored by ^{1}H NMR spectroscopy (300 MHz, $CDCl_3$, 6.5–7.5 ppm). Reaction condition: BPA-PC (508 mg, 2 mmol carbonate units), MeOH (3.2 g, 100 mmol, 50 equivalents relative to carbonate units), CO_2 (1 MPa), T = 140 °C.

Table 2 CO_2 catalyzed methanolysis of PET and BPA-PC pellets[a]

Entry	Material	Cat.	T (°C)	Conv. (%)	Selec. (%)
1	PET	N/A	200	N/A[b]	N/A[b]
2	PET	CO_2	200	100[c]	100[c]
3	PET	CO_2	170	N/A[b]	N/A[b]
4	BPA-PC	N/A	140	14[c]	92[c]
5	BPA-PC	CO_2	140	89[c]	90[c]
6	BPA-PC	CO_2	120	Trace[c]	N/A[b]

[a] Reaction conditions: each reaction was carried out in a 25 mL stainless-steel autoclave. PET pellets (384 mg, containing 4 mmol ester bonds), MeOH (3.2 g, 100 mmol, 25 equivalents relative to PET ester bonds) or BPA-PC pellets (508 mg, containing 2 mmol carbonate units), MeOH (3.2 g, 100 mmol, 50 equivalents relative to PC carbonate units), CO_2 (if any, 1 MPa), 6 h. [b] PET pellets could be observed visually. [c] Conversion and selectivity were determined by ^{1}H NMR spectroscopy (300 MHz, in $CDCl_3$).

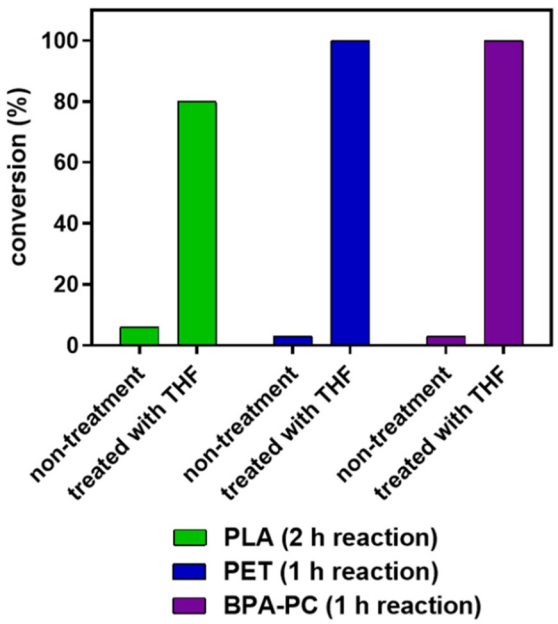

Fig. 5 Comparison of PLA, PET, and BPA-PC methanolysis under non-treatment and pre-treatment in THF conditions.

Open Access Article. Published on 31 October 2024. Downloaded on 1/15/2026 1:54:23 AM.
This article is licensed under a Creative Commons Attribution-NonCommercial 3.0 Unported Licence.

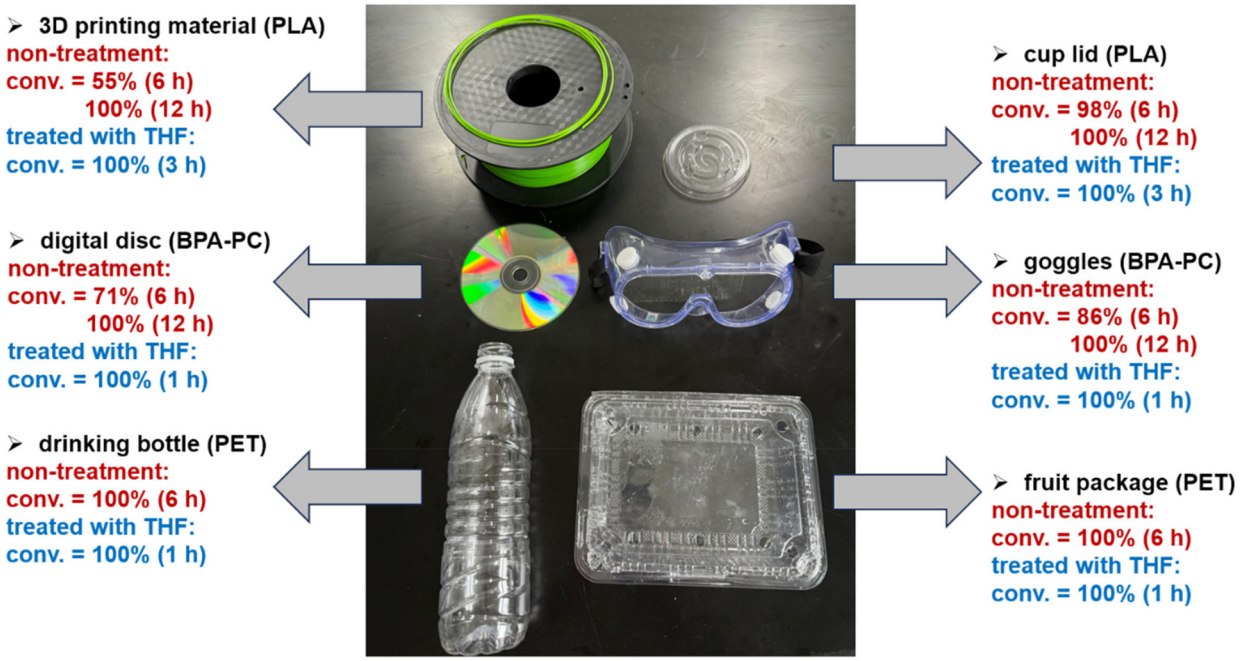

Fig. 6 Depolymerization of end-of-life materials.

pared to non-treatment materials. For instance, PLA methanolysis without solvent treatment yielded only 6% methyl lactate conversion after 2 hours, whereas pre-treatment increased conversion to 80%. Similarly, PET and BPA-PC required at least 6 hours for complete degradation without pre-treatment, but were fully depolymerized within 1 hour with pre-treatment. To sum up, pre-treatment polymeric materials with THF can largely enhance the rate of methanolysis.

Our protocol was also effective in depolymerizing end-of-life polyester and polycarbonate products. We selected 3D printing material (PLA), cup lids (PLA), digital disc (BPA-PC), goggles (BPA-PC), drinking bottles (PET), and food package (PET) as representative samples for CO_2-catalyzed methanolysis under both non-swelling and swelling conditions (Fig. 6). Complete conversion of these waste materials to the corresponding organic molecules were confirmed by ^{1}H NMR spectroscopy. The successful depolymerization of end-of-life plastics demonstrates the broad applicability of our CO_2 catalytic approach. Unlike conventional solid or liquid catalysts, CO_2 is a gaseous catalyst that readily dissipates upon autoclave opening, leaving no residue in the product. This eliminates the need for catalyst removal, streamlining the overall process.

Conclusions

In summary, this study explored the unconventional use of CO_2 as a standalone catalyst for the depolymerization of waste polyester and polycarbonate materials. Experimental and computational investigations, employing small molecule transesterification as a model, elucidated the catalytic mechanism of CO_2. The depolymerization process was determined to proceed *via* random scission of polymer chains. PLA, PET, and BPA-PC materials were successfully depolymerized through methanolysis, regardless of their molecular weight, shape, or other physical and chemical properties. Notably, CO_2 offers advantages over traditional solid or liquid catalysts by being inexpensive, non-toxic, metal-free, and residue-free. Beyond its established role as a C1 building block in synthetic chemistry, this research introduces CO_2 as a promising catalyst for sustainable chemistry, particularly in the context of waste polymer recycling and upcycling.

Data availability

The data supporting this article have been included as part of the ESI.†

Conflicts of interest

There are no conflicts to declare.

Acknowledgements

This work was financially supported by the National Natural Science Foundation of China, Fund for Distinguished Young Scholars (No. 52325301), CAS Project for Young Scientists in Basic Research (YSBR-094), and the National Natural Science Foundation of China, Basic Science Center Program (No. 51988102).

Open Access Article. Published on 31 October 2024. Downloaded on 1/15/2026 1:54:23 AM.
This article is licensed under a Creative Commons Attribution-NonCommercial 3.0 Unported Licence.

References

1 T. H. Epps, III, L. T. J. Korley, T. Yan, K. L. Beers and T. M. Burt, *JACS Au*, 2022, **2**, 3–11.
2 M. S. Kim, H. Chang, L. Zheng, Q. Yan, B. F. Pfleger, J. Klier, K. Nelson, E. L. W. Majumder and G. W. Huber, *Chem. Rev.*, 2023, **123**, 9915–9939.
3 A. Rahimi and J. M. García, *Nat. Rev. Chem.*, 2017, **1**, 0046.
4 J. M. Garcia and M. L. Robertson, *Science*, 2017, **358**, 870–872.
5 A. D. Vethaak and J. Legler, *Science*, 2021, **371**, 672–674.
6 J. M. Millican and S. Agarwal, *Macromolecules*, 2021, **54**, 4455–4469.
7 I. Vollmer, M. J. F. Jenks, M. C. P. Roelands, R. J. White, T. van Harmelen, P. de Wild, G. P. van der Laan, F. Meirer, J. T. F. Keurentjes and B. M. Weckhuysen, *Angew. Chem., Int. Ed.*, 2020, **59**, 15402–15423.
8 T. P. Haider, C. Völker, J. Kramm, K. Landfester and F. R. Wurm, *Angew. Chem., Int. Ed.*, 2019, **58**, 50–62.
9 C. Sun, S. Wei, H. Tan, Y. Huang and Y. Zhang, *Chem. Eng. J.*, 2022, **446**, 136881.
10 C. Jehanno, J. W. Alty, M. Roosen, S. De Meester, A. P. Dove, E. Y. X. Chen, F. A. Leibfarth and H. Sardon, *Nature*, 2022, **603**, 803–814.
11 R. Petrus, D. Bykowski and P. Sobota, *ACS Catal.*, 2016, **6**, 5222–5235.
12 L. A. Román-Ramírez, P. McKeown, M. D. Jones and J. Wood, *ACS Catal.*, 2019, **9**, 409–416.
13 P. McKeown, M. Kamran, M. G. Davidson, M. D. Jones, L. A. Román-Ramírez and J. Wood, *Green Chem.*, 2020, **22**, 3721–3726.
14 J. M. Payne, G. Kociok-Köhn, E. A. C. Emanuelsson and M. D. Jones, *Macromolecules*, 2021, **54**, 8453–8469.
15 F. Santulli, M. Lamberti and M. Mazzeo, *ChemSusChem*, 2021, **14**, 5470–5475.
16 R. Yang, G. Xu, B. Dong, X. Guo and Q. Wang, *ACS Sustainable Chem. Eng.*, 2022, **10**, 9860–9871.
17 M. Fuchs, P. M. Schäfer, W. Wagner, I. Krumm, M. Walbeck, R. Dietrich, A. Hoffmann and S. Herres-Pawlis, *ChemSusChem*, 2023, **16**, e202300192.
18 A. J. Spicer, A. Brandolese and A. P. Dove, *ACS Macro Lett.*, 2024, **13**, 189–194.
19 M. Brió Pérez, M. A. Hempenius, S. de Beer and F. R. Wurm, *Macromolecules*, 2023, **56**, 8856–8865.
20 M. Pérez-Venegas, T. Friščić and K. Auclair, *ACS Sustainable Chem. Eng.*, 2023, **11**, 9924–9931.
21 W. Wu, H. Zhai, K. Wu, X. Wang, W. Rao, J. Ding and L. Yu, *Chem. Eng. J.*, 2024, **480**, 148131.
22 S. Tian, Y. Jiao, Z. Gao, Y. Xu, L. Fu, H. Fu, W. Zhou, C. Hu, G. Liu, M. Wang and D. Ma, *J. Am. Chem. Soc.*, 2021, **143**, 16358–16363.
23 L. Shao, Y.-C. Chang, C. Hao, M.-e. Fei, B. Zhao, B. J. Bliss and J. Zhang, *Green Chem.*, 2022, **24**, 8716–8724.
24 F. Wu, Y. Wang, Y. Zhao, M. Tang, W. Zeng, Y. Wang, X. Chang, J. Xiang, B. Han and Z. Liu, *Sci. Adv.*, 2023, **9**, eade7971.
25 Y. Zhao, H. Zhang, F. Wu, R. Li, M. Tang, Y. Wang, W. Zeng, B. Han and Z. Liu, *Chem. Sci.*, 2024, **15**, 10892–10899.
26 S. Westhues, J. Idel and J. Klankermayer, *Sci. Adv.*, 2018, **4**, eaat9669.
27 R. Mi, L. Zeng, M. Wang, S. Tian, J. Yan, S. Yu, M. Wang and D. Ma, *Angew. Chem., Int. Ed.*, 2023, **62**, e202304219.
28 Y. Hu, S. Zhang, J. Xu, Y. Liu, A. Yu, J. Qian and Y. Xie, *Angew. Chem., Int. Ed.*, 2023, **62**, e202312564.
29 W. Zeng, Y. Zhao, F. Zhang, R. Li, M. Tang, X. Chang, Y. Wang, F. Wu, B. Han and Z. Liu, *Nat. Commun.*, 2024, **15**, 160.
30 M. Tang, J. Shen, Y. Wang, Y. Zhao, T. Gan, X. Zheng, D. Wang, B. Han and Z. Liu, *Nat. Commun.*, 2024, **15**, 5630.
31 C. S. M. Pereira, V. M. T. M. Silva and A. E. Rodrigues, *Green Chem.*, 2011, **13**, 2658–2671.
32 Y. Gu and F. Jérôme, *Chem. Soc. Rev.*, 2013, **42**, 9550–9570.
33 Q. Zhang, C. Hu, R. Duan, Y. Huang, X. Li, Z. Sun, X. Pang and X. Chen, *Green Chem.*, 2022, **24**, 9282–9289.
34 Q. Zhang, C. Hu, X. Pang and X. Chen, *ChemSusChem*, 2024, **17**, e202300907.
35 Q. Zhang, C. Hu, P.-Y. Li, F.-Q. Bai, X. Pang and X. Chen, *ACS Macro Lett.*, 2024, **13**, 151–157.
36 J. Artz, T. E. Müller, K. Thenert, J. Kleinekorte, R. Meys, A. Sternberg, A. Bardow and W. Leitner, *Chem. Rev.*, 2018, **118**, 434–504.
37 G. A. Bhat and D. J. Darensbourg, *Coord. Chem. Rev.*, 2023, **492**, 215277.
38 P. K. Sahoo, Y. Zhang and S. Das, *ACS Catal.*, 2021, **11**, 3414–3442.
39 G. Pupo, R. Properzi and B. List, *Angew. Chem., Int. Ed.*, 2016, **55**, 6099–6102.
40 M. Kapoor, D. Liu and M. C. Young, *J. Am. Chem. Soc.*, 2018, **140**, 6818–6822.
41 M. Kapoor, P. Chand-Thakuri and M. C. Young, *J. Am. Chem. Soc.*, 2019, **141**, 7980–7989.
42 J. Ye, I. Kalvet, F. Schoenebeck and T. Rovis, *Nat. Chem.*, 2018, **10**, 1037–1041.
43 J. Yang, W.-H. Li, H.-T. Tang, Y.-M. Pan, D. Wang and Y. Li, *Nature*, 2023, **617**, 519–523.
44 T. Roy, M. J. Kim, Y. Yang, S. Kim, G. Kang, X. Ren, A. Kadziola, H.-Y. Lee, M.-H. Baik and J.-W. Lee, *ACS Catal.*, 2019, **9**, 6006–6011.
45 M. Juhl, A. R. Petersen and J.-W. Lee, *Chem. – Eur. J.*, 2021, **27**, 228–232.
46 Y. Yang, J. Liu, F. S. Kamounah, G. Ciancaleoni and J.-W. Lee, *J. Org. Chem.*, 2021, **86**, 16867–16881.
47 H. Wang, Y. Li, S. Liu, M. Makha, J.-F. Bai and Y. Li, *ChemSusChem*, 2022, **15**, e202200227.
48 A. Kulkarni, G. Quintens and L. M. Pitet, *Macromolecules*, 2023, **56**, 1747–1758.
49 T. El Darai, A. Ter-Halle, M. Blanzat, G. Despras, V. Sartor, G. Bordeau, A. Lattes, S. Franceschi, S. Cassel, N. Chouini-Lalanne, E. Perez, C. Déjugnat and J.-C. Garrigues, *Green Chem.*, 2024, **26**, 6857–6885.
50 J. G. Kim, *Polym. Chem.*, 2020, **11**, 4830–4849.

 This journal is © The Royal Society of Chemistry 2024

Open Access Article. Published on 31 October 2024. Downloaded on 1/15/2026 1:54:23 AM.
This article is licensed under a Creative Commons Attribution-NonCommercial 3.0 Unported Licence.

51 T. Becker, A. Hermann, N. Saritas, A. Hoffmann and S. Herres-Pawlis, *ChemSusChem*, 2024, **17**, e202400933.
52 W. Leitner, *Acc. Chem. Res.*, 2002, **35**, 746–756.
53 S. Liu, L. Hu, J. Liu, Z. Zhang, H. Suo and Y. Qin, *Macromolecules*, 2024, **57**, 4662–4669.
54 Z.-X. Luo, G.-Q. Tian, S.-C. Chen, G. Wu and Y.-Z. Wang, *Macromolecules*, 2024, **57**, 6828–6837.
55 N. Fantozzi, J.-N. Volle, A. Porcheddu, D. Virieux, F. García and E. Colacino, *Chem. Soc. Rev.*, 2023, **52**, 6680–6714.
56 R. A. Sheldon, *Green Chem.*, 2023, **25**, 1704–1728.
57 R. A. Clark and M. P. Shaver, *Chem. Rev.*, 2024, **124**, 2617–2650.
58 C. Shi, E. C. Quinn, W. T. Diment and E. Y. X. Chen, *Chem. Rev.*, 2024, **124**, 4393–4478.
59 X. Bai, D. R. Aireddy, A. Roy and K. Ding, *Angew. Chem., Int. Ed.*, 2023, **62**, e202309949.
60 B. Ye, R. Zhou, Z. Zhong, S. Wang, H. Wang and Z. Hou, *Green Chem.*, 2023, **25**, 7243–7252.
61 T. Do, E. R. Baral and J. G. Kim, *Polymer*, 2018, **143**, 106–114.
62 E. Luna, I. Olazabal, M. Roosen, A. Müller, C. Jehanno, M. Ximenis, S. de Meester and H. Sardon, *Chem. Eng. J.*, 2024, **482**, 148861.